

# Models of magnetized neutron star atmospheres

V. Suleimanov<sup>a,b,\*</sup>, A.Y. Potekhin<sup>c</sup>, K. Werner<sup>a</sup>

<sup>a</sup>*Institut für Astronomie und Astrophysik, Kepler Center for Astro and Particle Physics, Universität Tübingen, Sand 1, 72076 Tübingen, Germany*

<sup>b</sup>*Kazan State University, Kremlevskaja Street, 18, Kazan 420008, Russia*

<sup>c</sup>*Ioffe Physical-Technical Institute, Polytekhnicheskaya Street, 26, St. Petersburg 194021, Russia*

Received 20 April 2009; received in revised form 11 August 2009; accepted 22 August 2009

## Abstract

We present a new computer code for modeling magnetized neutron star atmospheres in a wide range of magnetic fields ( $10^{12}$ – $10^{15}$  G) and effective temperatures ( $3 \times 10^5$ – $10^7$  K). The atmosphere is assumed to consist either of fully ionized electron-ion plasmas or of partially ionized hydrogen. Vacuum resonance and partial mode conversion are taken into account. Any inclination of the magnetic field relative to the stellar surface is allowed. We use modern opacities of fully or partially ionized plasmas in strong magnetic fields and solve the coupled radiative transfer equations for the normal electromagnetic modes in the plasma. Using this code, we study the possibilities to explain the soft X-ray spectra of isolated neutron stars by different atmosphere models. In particular, the outgoing spectrum using the “sandwich” model (thin atmosphere with a hydrogen layer above a helium layer) is constructed. Thin partially ionized hydrogen atmospheres with vacuum polarization are shown to be able to improve our understanding of the observed spectrum of the nearby isolated neutron star RBS 1223 (RX J1308.8+2127).

© 2009 COSPAR. Published by Elsevier Ltd. All rights reserved.

**Keywords:** Radiative transfer; Numerical; Neutron stars; Atmospheres; X-rays; Individual: RX J1308.8+2127

## 1. Introduction

At present several classes of neutron stars (NSs) with strong magnetic field are known. They include X-ray dim isolated NSs (XDINSs, Haberl, 2007), central compact objects (CCOs) in supernova remnants (Pavlov et al., 2004), anomalous X-ray pulsars and soft-gamma repeaters (AXPs and SGRs; see reviews by Kaspi, 2007; Mereghetti et al., 2007; Mereghetti, 2008). The NSs in these classes have superstrong magnetic fields up to  $B \geq 10^{14}$  G (SGR and AXP) and  $B \sim$  a few  $\times 10^{13}$  G in XDINSs, evaluated from period changes and from absorption features in the observed spectra, if they are interpreted as ion cyclotron lines (see reviews by Haberl, 2007; van Kerkwijk and Kaplan, 2007).

These NSs are sufficiently hot ( $T_{\text{eff}} \sim 10^6$ – $10^7$  K) to be observed as thermal soft X-ray sources. Some of the XDINSs and CCOs have one or more absorption features in their X-ray spectrum at the energies 0.2–0.8 keV (Haberl, 2007), and the central energies of these features appear to be harmonically spaced (Sanwal et al., 2002; Bignami et al., 2003; Schwöpe et al., 2007; van Kerkwijk and Kaplan, 2007; Haberl, 2007). The optical/ultraviolet fluxes of the known XDIN optical counterparts are a few times larger than the blackbody extrapolation of the X-ray spectra (Burwitz et al., 2001; Burwitz et al., 2003; Kaplan et al., 2003; Motch et al., 2003; Mignani et al., 2007).

The XDINs are nearby objects, and parallaxes of some of them have been measured (Kaplan et al., 2002a). Therefore, they give a good possibility to measure the NS radii, yielding useful information on the equation of state (EOS) for the NS inner core (Trümper et al., 2004; Lattimer and Prakash, 2007). For a sufficiently accurate evaluation of NS radii, a good model of the NS surface radiation is necessary for the observed X-ray spectra fitting.

\* Corresponding author. Address: Institut für Astronomie und Astrophysik, Kepler Center for Astro and Particle Physics, Universität Tübingen, Sand 1, 72076 Tübingen, Germany.

E-mail address: [suleimanov@astro.uni-tuebingen.de](mailto:suleimanov@astro.uni-tuebingen.de) (V. Suleimanov).

Structures and emergent spectra of NS atmospheres with strong ( $B \geq 10^{12}$  G) magnetic fields have been modeled by many scientific groups (Shibanov et al., 1992; Rajagopal et al., 1997; Özel, 2001; Ho and Lai, 2001, 2003, 2004; van Adelsberg and Lai, 2006). Methods of fully ionized model atmospheres modeling (see, e.g., Zavlin, 2009 for references) and partially ionized hydrogen atmospheres modeling (Potekhin et al., 2004; Ho and Lai, 2004; Ho et al., 2008) were developed. Mid-Z element atmospheres for strongly magnetized NSs have also been modeled (Mori and Ho, 2007). The effect of the vacuum polarization on magnetized NS atmospheres was studied by Pavlov and Gnedin (1984) and Lai and Ho (2002, 2003), and model atmospheres with partial mode conversion due to vacuum polarization have been computed (Ho and Lai, 2003; van Adelsberg and Lai, 2006). Some of the XDINSs might have a “thin” atmosphere above the condensed surface, which could be optically thick to low-energy photons and optically thin to high-energy photons (Motch et al., 2003; Ho et al., 2007).

Here we present a new computer code, which allows to compute magnetized NS model atmospheres consisting of partially ionized hydrogen, taking into account the vacuum polarization effect together with partial mode conversion and an arbitrary magnetic field inclination. Compared to previous codes, other methods were used for the temperature correction procedure and the solution of the radiation transfer equation. We also present some new results, which were obtained by using this code.

## 2. Method of atmosphere structure calculations

We computed model atmospheres of hot, magnetized NSs subject to the constraints of hydrostatic and radiative equilibrium assuming planar geometry. There are two versions of the code: the first one is designed for the magnetic field  $\mathbf{B}$  perpendicular to the surface, and in the second version, the angle  $\theta_B$  between  $\mathbf{B}$  and  $\mathbf{n}$  is arbitrary, and calculations are more expensive.

The model atmosphere structure for an NS with effective temperature  $T_{\text{eff}}$ , surface gravity  $g$ , magnetic field  $\mathbf{B}$ , and given chemical composition is described by a set of equations (e.g., Shibanov et al., 1992; Ho and Lai, 2001 and references therein), which are written below for the simplest first case, where  $\theta_B = 0$ . In the second case (for arbitrary  $\theta_B$ , e.g., Zavlin et al., 1995), there is an additional dependence of the absorption ( $k_v^i$ ) and scattering ( $\sigma_v^i$ ) coefficients on the azimuthal angle  $\varphi$ ; accordingly, there are additional integrations over  $\varphi$  in Eqs. (3), (6), (8) and (9) in the second case.

The hydrostatic equilibrium equation reads

$$\frac{dP_g}{dm} = g - g_{\text{rad}}, \quad (1)$$

where

$$g = \frac{GM_{\text{NS}}}{R_{\text{NS}}^2 \sqrt{1 - R_S/R_{\text{NS}}}}, \quad (2)$$

$$g_{\text{rad}} = \frac{2\pi}{c} \sum_{i=1}^2 \int_0^\infty dv \int_{-1}^{+1} (k_v^i + \sigma_v^i) \mu I_v^i(\mu) d\mu, \quad (3)$$

and  $R_S = 2GM_{\text{NS}}/c^2$  is the Schwarzschild radius.  $I_v^i(\mu)$  is the specific intensity in mode  $i$ ,  $\mu = \cos \theta$ , where  $\theta$  is the angle between the surface normal and the radiation propagation direction,  $P_g$  is the gas pressure, and the column density  $m$  is determined as

$$dm = -\rho dz. \quad (4)$$

The variable  $\rho$  denotes the gas density and  $z$  is the vertical distance.

The radiation transfer equations for the two modes are

$$\mu \frac{dI_v^i}{d\tau_v^i} = I_v^i - S_v^i \quad (5)$$

where the source function is

$$S_v^i = \frac{k_v^i}{k_v^i + \sigma_v^i} \frac{B_v}{2} + \frac{1}{k_v^i + \sigma_v^i} \times \sum_{j=1}^2 \int_{-1}^{+1} \sigma_v^{ij}(\mu, \mu') I_v^j(\mu') d\mu', \quad (6)$$

and  $B_v$  is the blackbody (Planck) intensity. The optical depth  $\tau_v^i$  is defined as

$$d\tau_v^i = (k_v^i + \sigma_v^i) dm. \quad (7)$$

Of course, opacities  $k_v^i$  and  $\sigma_v^i$  depend on  $\mu$ . These equations have to be completed by the energy balance equation

$$\int_0^\infty dv \sum_{i=1}^2 \int_{-1}^{+1} ((k_v^i + \sigma_v^i) I_v^i(\mu) - \eta_v^i(\mu)) d\mu = 0 \quad (8)$$

with emissivity

$$\eta_v^i(\mu) = k_v^i \frac{B_v}{2} + \sum_{j=1}^2 \int_{-1}^{+1} \sigma_v^{ij}(\mu, \mu') I_v^j(\mu') d\mu', \quad (9)$$

Eqs. (1)–(9) must be completed by the EOS and the charge and particle conservation laws. In the code two different cases of these laws are considered.

In the first (simplest) case, a fully ionized atmosphere is calculated. Therefore, the EOS is the ideal gas law

$$P_g = n_{\text{tot}} kT, \quad (10)$$

where  $n_{\text{tot}}$  is the number density of all particles. Opacities are calculated in the same way as in the paper by van Adelsberg and Lai (2006) (see references therein for the background theory and more sophisticated approaches). The vacuum polarization effect is taken into account following the same work.

The second considered case is a partially ionized hydrogen atmosphere. In this case the EOS and the corresponding opacities are taken from tables calculated by Potekhin and Chabrier (2003, 2004). The normal mode polarization vectors are taken from the calculations by Potekhin et al. (2004). The vacuum polarization effect is also included.

We use a logarithmically equidistant photon energy set in our computations in the range 0.001–20 keV with additional points near each ion cyclotron resonance. If the vacuum resonance is taken into consideration, then another photon energy grid is used, which is constructed using the “equal grid” method (Ho and Lai, 2003). This energy grid is recalculated after every iteration.

The radiation transfer Eq. (5) is solved on a set of 40 polar angles  $\theta$  (and additionally 6 azimuthal angles  $\varphi$  in the case of inclined magnetic field) by the short characteristic method (Olson and Kunasz, 1987). We use the conventional condition (no external radiation) at the outer boundary. At the inner boundary we take the incoming specific intensities equal to blackbody radiation corresponding to the temperature of the last atmosphere point. In the case of the thin atmosphere the temperature at the inner boundary is considered as the temperature of a condensed NS surface. The code allows one to take into account the partial mode conversion according to van Adelsberg and Lai (2006).

The solution of the radiative transfer Eq. (5) is checked for the energy balance Eq. (8). Temperature corrections are then evaluated using three different procedures (Kurucz, 1970), modified to deal with strong magnetic fields. A non-magnetic version of this code was described, for example, by Ibragimov et al. (2003) and Suleimanov and Werner (2007).

The iteration procedure is repeated until the relative flux error is smaller than 1% and the relative flux derivative error is smaller than 0.01%.

Our method of calculation has been tested by a comparison to models for magnetized NS atmospheres (Shibanov et al., 1992; Pavlov et al., 1994; Ho and Lai, 2001; Özel, 2001; Ho and Lai, 2003). Model atmospheres with partially ionized hydrogen are compared to models computed by Ho et al. (2007). We have found that our models are in a good agreement with these calculations.

### 3. Results

Here we present some new results, obtained by using of the developed code. In all calculations below we use the same surface gravity,  $\log g = 14.3$ .

One of the problems related to AXPs is the lack of any absorption feature at the proton cyclotron energy. Ho and Lai (2003) suggested that a possible solution of this problem is the suppression of the cyclotron absorption feature due to the vacuum polarization. We demonstrate that this absorption line is also further reduced in a thin atmosphere. Fig. 1 demonstrates emergent spectra of thin atmospheres without allowance for the vacuum polarization effect. The absorption feature disappears with decreasing the atmosphere surface density  $\Sigma$ . Equivalent widths of the absorption feature are  $\approx 670$  eV for the semi-infinite atmosphere,  $\approx 190$  eV for the  $\Sigma = 100$  g cm $^{-2}$  slab and  $\approx 5$  eV for the  $\Sigma = 1$  g cm $^{-2}$  slab. This decrease of the

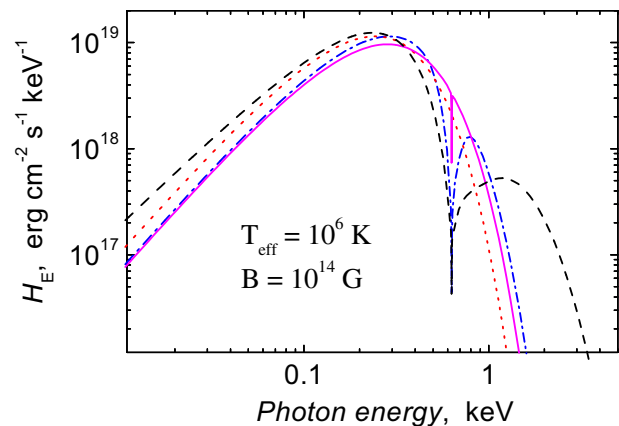


Fig. 1. Emergent spectra of the thin fully ionized hydrogen atmospheres above a solid surface with  $T_{\text{eff}} = 10^6$  K and  $B = 10^{14}$  G in comparison to the semi-infinite atmosphere (dashed curve). The spectra of atmospheres with surface densities  $\Sigma = 1$  (solid curve) and  $100$  g cm $^{-2}$  (dash-dotted curve) together with the corresponding blackbody (dotted curve) are shown.

equivalent width corresponds to the decrease of the optical depth according to the curve of growth.

Various hypotheses were considered for an explanation of the two harmonically spaced absorption features in CCOs (see Mori and Ho, 2007 and references therein). Here we suggest another one, which we name “sandwich atmosphere”. A thin, chemically layered atmosphere above a condensed NS surface can arise from accretion of interstellar gas with cosmic chemical composition. In this case, hydrogen and helium quickly separate due to the high gravity. In this “sandwich atmosphere” a layer of hydrogen is located above a helium slab, and the emergent spectrum has two absorption features, corresponding to proton and  $\alpha$ -particle cyclotron energies. In Fig. 2 the emergent spectrum for one of such models together with the corresponding temperature structure are shown. Fully ionized hydrogen and helium layers are considered in this model. The emission feature at the helium absorption line arises due to a local temperature bump at the boundary between the helium and hydrogen layers. This temperature increase compensates a lower number density in the hydrogen layer to avoid a gas pressure jump. Of course, this temperature jump should be smoothed by hydrogen-helium mixing and thermal conduction flux at the boundary between layers. Here we used the sharp boundary and did not take into account thermal conductivity. Results can also change quantitatively, if partially ionized hydrogen and helium layers are considered.

Most of the XDINSs have magnetic fields  $B \geq 10^{13}$  G and color temperatures  $\approx 10^6$  K (Haberl, 2007). Hydrogen model atmospheres are partially ionized under these conditions and the vacuum polarization effect is also significant. Here we present first results of modeling of partially ionized hydrogen atmospheres with the vacuum polarization effect and partial mode conversion using our radiative transfer code. Previously partial mode conversion was con-

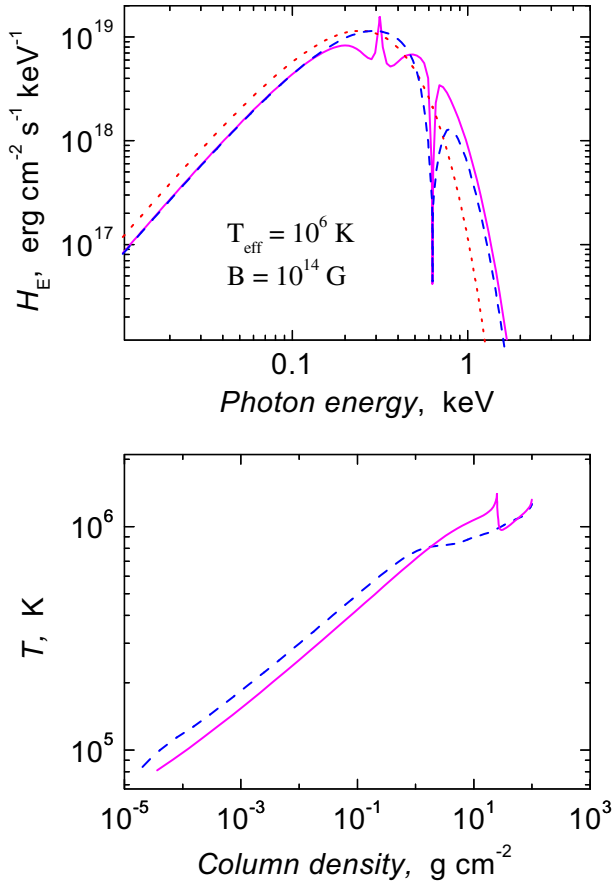


Fig. 2. Emergent spectrum (top panel) and temperature structure (bottom panel) of the “sandwich” model atmosphere above a solid surface with  $T_{\text{eff}} = 10^6$  K and  $B = 10^{14}$  G (solid curve) in comparison with the thin fully ionized hydrogen atmosphere (dashed curve) with the same parameters. The surface densities of both model atmospheres are  $100 \text{ g cm}^{-2}$ , in the “sandwich” model the H slab has  $25 \text{ g cm}^{-2}$  surface density and the He slab has  $75 \text{ g cm}^{-2}$ . The corresponding blackbody spectrum (dotted curve) is also shown in the top panel.

sidered only for fully ionized atmosphere models (van Adelsberg and Lai, 2006). In Fig. 3 we compare spectra and temperature structures of the partially ionized hydrogen model atmospheres with and without the partial mode conversion effect. When the X-mode (having smaller opacity) partially converts to the O-mode in the surface layers of the atmosphere, the energy absorbed by the O-mode heats these upper layers. As a result, the emergent spectra are closer to the blackbody. The absorption feature to the right of the proton cyclotron line arises mainly due to the transition from the ground state to the first excited state of the H atom; it has a maximum at 350 eV and is strongly broadened at lower energies because of the atomic motion effect (cf. Fig. 5 in Potekhin and Chabrier, 2004 and related discussion there).

The effective temperature and magnetic field strengths are not uniform over the NS surface, and generally the magnetic field is not perpendicular to the surface. Therefore, for comparison to observations, it will be necessary to integrate the local model spectra over the NS surface

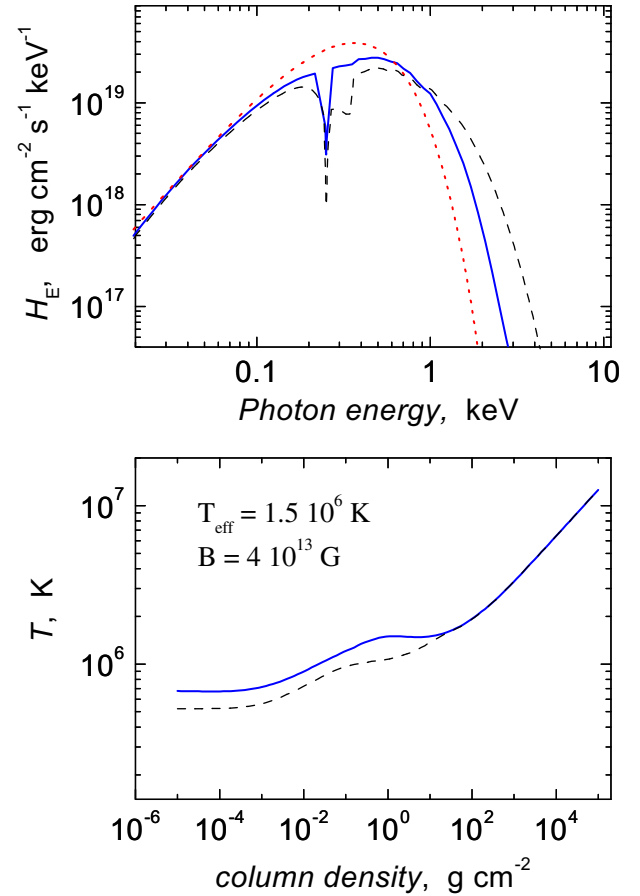


Fig. 3. Emergent spectra and temperature structures of the partially ionized hydrogen model atmospheres with  $T_{\text{eff}} = 1.5 \times 10^6$  K with (solid curves) and without (dashed curves) vacuum polarization effect (with the partial mode conversion). The magnetic field strength is  $B = 4 \times 10^{13}$  G. The corresponding blackbody spectrum is also shown in the upper panel (dotted curve).

(see Zavlin et al., 1995; Ho et al., 2008), and to compute model atmospheres with inclined magnetic field. This possibility is included in our code. For example, Fig. 4 shows spectra and temperature structures of partially ionized hydrogen model atmospheres with magnetic field perpendicular and parallel to the NS surface. The vacuum polarization effect is taken into account without mode conversion. The difference between emergent spectra is not significant (see also the first models with different magnetic field inclinations in Kaminker et al., 1982; Shibano et al., 1992), but it can be more significant at other atmospheric parameters (Ho et al., 2008).

Ho et al. (2007) demonstrated that a single partially ionized thin hydrogen atmosphere can explain the problem of the observed optical/UV flux excess over the blackbody extrapolation from X-ray to the optical range in the case of brightest isolated NS RXJ1856.4–3754: the model fits well both the observed optical flux and the X-ray spectrum. RXJ1856.4–3754 has very low pulsed fraction of radiation ( $\approx 1.2\%$ , Tiengo and Mereghetti, 2007), therefore it is possible to fit the radiation of this star by a single model

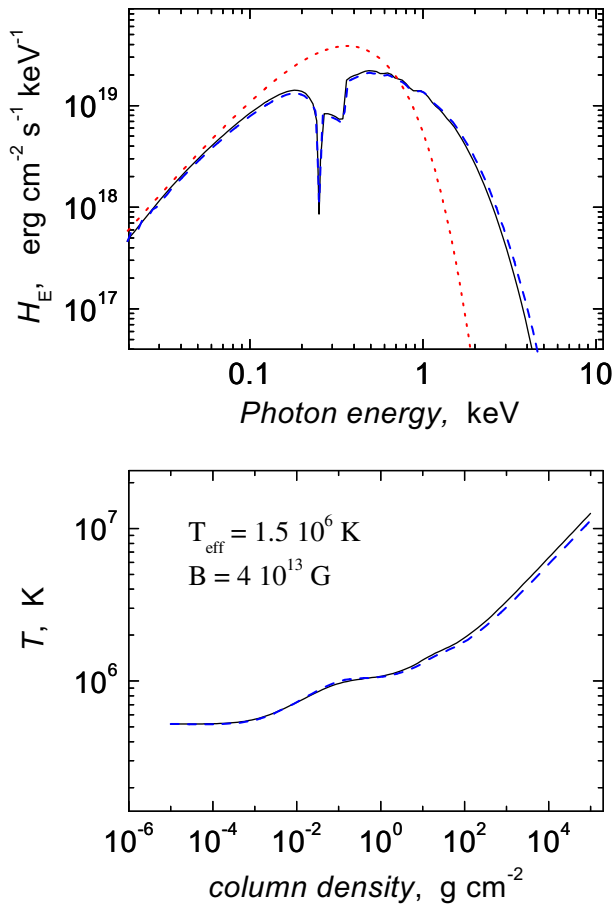


Fig. 4. Emergent spectra and temperature structures of partially ionized hydrogen model atmospheres with  $T_{\text{eff}} = 1.5 \times 10^6$  K with inclinations of the magnetic field ( $B = 4 \times 10^{13}$  G) to the surface normal  $\theta_B$  equal  $0^\circ$  (solid curves) and  $90^\circ$  (dashed curves). The vacuum polarization effect is not included. The corresponding blackbody spectrum is also shown in the upper panel (dotted curve).

atmosphere (although the small pulsed fraction can also be explained by a small value of an angle between the magnetic and rotation axes or between the rotation axis and the line of sight). Other XDINSs have larger pulse fractions, up to 18% (RBS 1223, Haberl et al., 2004). In this case the temperature is certainly not uniform across the NS surface, and the excess optical flux can be explained by the radiation from cool surface parts (Schwope et al., 2005).

We now investigate properties of partially ionized hydrogen models, which can be applied to the RBS 1223 atmosphere. The color temperature of this star, found from X-ray spectra fitting, is close to  $10^6$  K, with magnetic field  $B \approx 4 \times 10^{13}$  G (Schwope et al., 2007). In particular, we study the optical flux excess in comparison to the X-ray fitted blackbody flux in this kind of models in order to explore which part of the observed optical excess can be explained by the atmosphere effect. This optical excess is illustrated in the top panel of Fig. 6. For this aim we have calculated two sets of models with vacuum polarization and partial mode conversion. The models in the first set have effective temperatures

$T_{\text{eff}} = 10^6$  K and the models of second one have effective temperatures  $T_{\text{eff}} = 1.2 \times 10^6$  K. In both sets  $B = 4 \times 10^{13}$  G, and models with surface densities  $\Sigma = 1, 3, 10, 30, 100$  and  $10^5$  (semi-infinite model)  $\text{g cm}^{-2}$  are computed. In Fig. 5 we show emergent spectra and temperature structures for some models from the second set. Clearly, the X-ray spectra of the models with  $\Sigma \leq 10 \text{ g cm}^{-2}$  are close to a blackbody and, therefore, better fit the observed X-ray spectrum. Let us remark that there is a significant absorption feature in the RBS 1223 spectrum (Schwope et al., 2007), which cannot be fitted by the simple blackbody spectrum. Here we do not try to fit the observed spectrum of RBS 1223 by the single temperature model: clearly, such fitting would require the integration of the local spectra over the neutron star surface assuming some non-uniform temperature and a magnetic field distributions (see Zavlin et al., 1995; Ho et al., 2008). Instead, we are trying to understand, what kind of atmosphere (thin or semi-infinite) be more appropriate for this modeling.

In Fig. 6 (bottom panel) we show the ratio of the model atmosphere flux to the X-ray fitted (in the 0.4–1 keV

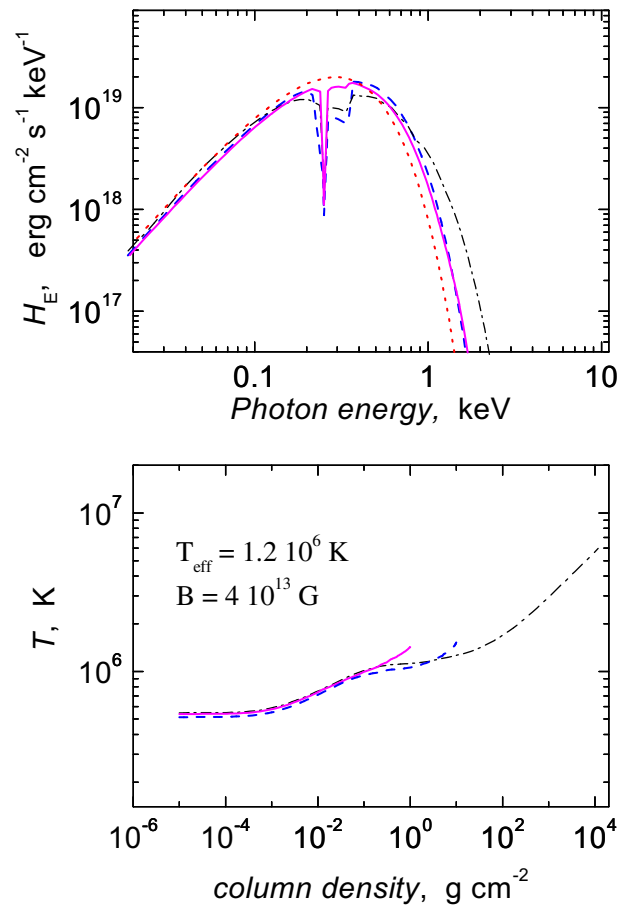


Fig. 5. Emergent spectra and temperature structures of the partially ionized hydrogen model atmospheres with  $T_{\text{eff}} = 1.2 \times 10^6$  K with vacuum polarization effect and partial mode conversion shown for various surface densities  $\Sigma$  (solid curves –  $1 \text{ g cm}^{-2}$ , dashed curves –  $10 \text{ g cm}^{-2}$ , dash-dotted curves – semi-infinite atmosphere). The magnetic field strength is  $B = 4 \times 10^{13}$  G. The corresponding blackbody spectrum is also shown in the upper panel (dotted curve).

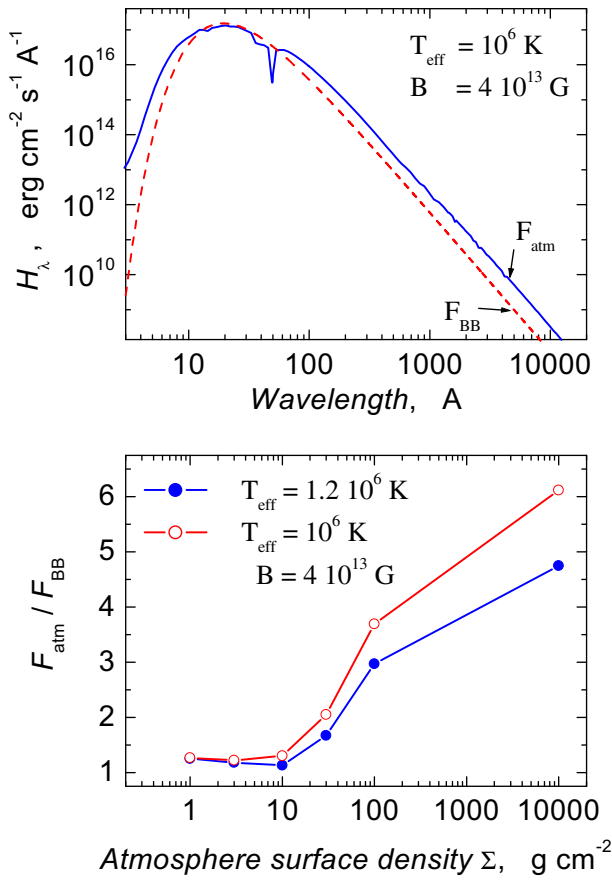


Fig. 6. *Top panel:* Emergent spectrum of the partially ionized hydrogen model atmosphere of neutron stars with  $T_{\text{eff}} = 10^6$  K with vacuum polarization effect, partial mode conversion and magnetic field strength  $B = 4 \times 10^{13}$  G. The blackbody spectrum fitted to the maximum of the spectral distribution is also shown (dashed curve). At the optical band the model atmosphere flux is a few times larger than the blackbody flux. *Bottom panel:* Ratios of the model atmosphere flux to the blackbody (X-ray fitted) flux at the optical band depending on the model atmosphere thickness (surface density  $\Sigma$ ) for the models with  $T_{\text{eff}} = 10^6$  K and  $T_{\text{eff}} = 1.2 \times 10^6$  K.

range) blackbody flux in the optical band at  $\lambda = 5150$  Å depending on  $\Sigma$  for both sets. The observed ratio is about 5 (Kaplan et al., 2002b), in agreement with the semi-infinite atmosphere models. However, the observed blackbody like X-ray spectrum agrees with the thin atmosphere models, for which this ratio is close to 1. Therefore, the observed optical excess cannot be explained by the thin atmosphere model alone; instead, it can arise due to a nonuniform surface temperature distribution, in agreement with the RBS 1223 light curve modeling (Schwope et al., 2005).

#### 4. Conclusions

In this work we present a new code, which can model fully ionized and partially ionized hydrogen atmospheres in a wide range of effective temperatures ( $3 \times 10^5 - 10^7$  K) and magnetic fields ( $10^{12} - 10^{15}$  G), with any inclination of the magnetic field to the stellar surface. The vacuum polarization effect with partial mode conversion is taken

into consideration. Calculated emergent spectra and temperature structures of the model atmospheres agree with previously published ones.

We have studied the properties of thin atmospheres above condensed NS surfaces. We demonstrated that the proton cyclotron absorption line disappears in the thin hydrogen model atmospheres. A new thin “sandwich” model atmosphere (hydrogen layer above helium layer) is proposed to explain the occurrence of two absorption features in the observed X-ray spectra of some isolated NSs.

A set of partially ionized hydrogen model atmospheres with vacuum polarization and partial mode conversion with parameters (effective temperature and the magnetic field strength) close to the probable parameters of the isolated NS RBS 1223 were calculated. We analysed the optical excess (relative to the X-ray fitted blackbody flux) in the model spectra and found that the optical flux excess  $\approx 5$  for the semi-infinite model atmospheres decreases down to 1 with decreasing surface density  $\Sigma$  of the atmosphere. Spectra of thin model atmospheres are closer to the observed RBS 1223 X-ray spectrum, therefore we conclude that the observed optical excess should be explained by nonuniform surface temperature distribution.

#### Acknowledgements

VS thanks DFG for financial support (Grant We 1312/35-1 and Grant SFB/Transregio 7 “Gravitational Wave Astronomy”) and the President’s programme for support of leading science schools (Grant NSH-4224.2008.2). The work of AYP is supported by RFBR Grant 08-02-00837 and the President’s programme for support of leading science schools (Grant NSH-2600.2008.2).

#### References

- Bignami, G.F., Caraveo, P.A., De Luca, A., Mereghetti, S. The magnetic field of an isolated neutron star from X-ray cyclotron absorption lines. *Nature* 423, 725–727, 2003.
- Burwitz, V., Zavlin, V.E., Neuhäuser, R., et al. The Chandra LETGS high resolution X-ray spectrum of the isolated neutron star RX J1856.5–3754. *A&A* 379, L35–L38, 2001.
- Burwitz, V., Haberl, F., Neuhäuser, R., et al. The thermal radiation of the isolated neutron star RX J1856.5–3754 observed with Chandra and XMM-Newton. *A&A* 399, 1109–1114, 2003.
- Haberl, F., Motch, C., Zavlin, V.E., et al. The isolated neutron star X-ray pulsars RX J0420.0–5022 and RX J0806.4–4123: new X-ray and optical observations. *A&A* 424, 635–645, 2004.
- Haberl, F. The magnificent seven: magnetic fields and surface temperature distributions. *A&SS* 308, 181–190, 2007.
- Ho, W.C.G., Lai, D. Atmospheres and spectra of strongly magnetized neutron stars. *MNRAS* 327, 1081–1096, 2001.
- Ho, W.C.G., Lai, D. Atmospheres and spectra of strongly magnetized neutron stars – II. The effect of vacuum polarization. *MNRAS* 338, 233–252, 2003.
- Ho, W.C.G., Lai, D. Spectral features in the thermal emission from isolated neutron stars: dependence on magnetic field strengths. *ApJ* 607, 420–425, 2004.
- Ho, W.C.G., Kaplan, D.L., Chang, P., van Adelsberg, M., Potekhin, A.Y. Magnetic hydrogen atmosphere models and the neutron star RX J1856.5–3754. *MNRAS* 375, 821–830, 2007.

- Ho, W.C.G., Potekhin, A.Y., Chabrier, G. Model X-ray spectra of magnetic neutron stars with hydrogen atmospheres. *ApJ Suppl. Ser.* 178, 102–109, 2008.
- Ibragimov, A.A., Suleimanov, V.F., Vikhlinin, A., Sakhibullin, N.A. Supersoft X-ray Sources. Parameters of Stellar Atmospheres. *Astron. Rep.* 47, 186–196, 2003.
- Kaminker, A.D., Pavlov, G.G., Shibanov, Yu.A. Radiation for a strongly-magnetized plasma – The case of predominant scattering. *Astroph. Space Sci.* 86, 249–297, 1982.
- Kaplan, D.L., van Kerkwijk, M.H., Anderson, J. The Parallax and Proper Motion of RX J1856.5–3754 Revisited. *ApJ* 571, 447–457, 2002a.
- Kaplan, D.L., Kulkarni, S.R., van Kerkwijk, M.H. A Probable optical counterpart to the isolated neutron star RX J1308.6+2127. *ApJ* 579, L29–L32, 2002b.
- Kaplan, D.L., van Kerkwijk, M.H., Marshall, H.L., et al. The Nearby Neutron Star RX J0720.4–3125 from Radio to X-rays. *ApJ* 590, 1008–1019, 2003.
- Kaspi, V.M. Recent progress on anomalous X-ray pulsars. *A&SS* 308, 1–11, 2007.
- Kurucz, R.L. Atlas: a computer program for calculating model stellar atmospheres. *SAO Special Report* 309, 1970.
- Lai, D., Ho, W.C.G. Resonant conversion of photon modes due to vacuum polarization in a magnetized plasma: implications for X-ray emission from magnetars. *ApJ* 566, 373–377, 2002.
- Lai, D., Ho, W.C.G. Transfer of polarized radiation in strongly magnetized plasmas and thermal emission from magnetars: effect of vacuum polarization. *ApJ* 588, 962–974, 2003.
- Lattimer, J.M., Prakash, M. Neutron star observations: prognosis for equation of state constraints. *Phys. Rep.* 442, 109–165, 2007.
- Mereghetti, S. The strongest cosmic magnets: soft gamma-ray repeaters and anomalous X-ray pulsars. *A&A Rev.* 15, 225–287, 2008.
- Mereghetti, S., Esposito, P., Tiengo, A. XMM Newton observations of soft gamma-ray repeaters. *A&SS* 308, 13–23, 2007.
- Mignani, R.P., Bagnulo, S., De Luca, A., et al. Studies of neutron stars at optical/IR wavelengths. *A&SS* 308, 203–210, 2007.
- Mori, K., Ho, W.C.G. Modelling mid-Z element atmospheres for strongly magnetized neutron stars. *MNRAS* 377, 905–919, 2007.
- Motch, C., Zavlin, V.E., Haberl, F. The proper motion and energy distribution of the isolated neutron star RX J0720.4–3125. *A&A* 408, 323–330, 2003.
- Olson, G.L., Kunasz, P.B. Short characteristic solution of the non-LTE transfer problem by operator perturbation. I. The one-dimensional planar slab. *JQSRT* 38, 325–336, 1987.
- Özel, F. Surface emission properties of strongly magnetic neutron stars. *ApJ* 563, 276–288, 2001.
- Pavlov, G.G., Gnedin, Yu.N. Vacuum polarization by a magnetic field and its astrophysical manifestations. *Astrophys. Space Phys. Rev.* 3, 197–253, 1984.
- Pavlov, G.G., Shibanov, Yu.A., Ventura, J., Zavlin, V.E. Model atmospheres and radiation of magnetic neutron stars: anisotropic thermal emission. *A&A* 289, 837–845, 1994.
- Pavlov, G.G., Sanwal, D., Teter, M.A.. Central Compact Objects in Supernova Remnants. In: Camilo, F., Gaensler, B.M. (Eds.), *Young Neutron Stars and Their Environments* (Proceedings of the IAU Symp. 218), ASP, San Francisco, 239–246, 2004.
- Potekhin, A.Y., Chabrier, G. Equation of state and opacities for hydrogen atmospheres of neutron stars with strong magnetic fields. *ApJ* 585, 955–974, 2003.
- Potekhin, A.Y., Chabrier, G. Equation of state and opacities for hydrogen atmospheres of magnetars. *ApJ* 600, 317–323, 2004.
- Potekhin, A.Y., Lai, D., Chabrier, G., Ho, W.C.G. Electromagnetic polarization in partially ionized plasmas with strong magnetic fields and neutron star atmosphere models. *ApJ* 612, 1034–1043, 2004.
- Rajagopal, M., Romani, R.W., Miller, M.C. Magnetized iron atmospheres for neutron stars. *ApJ* 479, 347–356, 1997.
- Sanwal, D., Pavlov, G.G., Zavlin, V.E., et al. Discovery of absorption of an isolated neutron star. *ApJ* 574, L61–L64, 2002.
- Schwöpe, A.D., Hambaryan, V., Haberl, F., et al. The pulsed X-ray light curves of the isolated neutron star RBS1223. *A&A* 441, 597–604, 2005.
- Schwöpe, A.D., Hambaryan, V., Haberl, F., Motch, C. The complex X-ray spectrum of the isolated neutron star RBS1223. *A&S* 308, 619–623, 2007.
- Shibanov, I.A., Zavlin, V.E., Pavlov, G.G., Ventura, J. Model atmospheres and radiation of magnetic neutron stars. I – The fully ionized case. *A&A* 266, 313–320, 1992.
- Suleimanov, V., Werner, K. Importance of Compton scattering for radiation spectra of isolated neutron stars with weak magnetic fields. *A&A* 466, 661–666, 2007.
- Tiengo, A., Mereghetti, S. XMM-Newton discovery of 7 s pulsations in the isolated neutron star RX J1856.5–3754. *ApJ* 657, L101–L104, 2007.
- Trümper, J.E., Burwitz, V., Haberl, F., Zavlin, V.E. The puzzles of RX J1856.5–3754: neutron star or quark star? *Nucl. Phys. B Proc. Suppl.* 132, 560–565, 2004.
- van Adelsberg, M., Lai, D. Atmosphere models of magnetized neutron stars: QED effects, radiation spectra and polarization signals. *MNRAS* 373, 1495–1522, 2006.
- van Kerkwijk, M.H., Kaplan, D.L. Isolated neutron stars: magnetic fields, distances, and spectra. *A&SS* 308, 191–201, 2007.
- Zavlin, V.E., Pavlov, G.G., Shibanov, Y.A., Ventura, J. Thermal radiation from rotating neutron star: effect of the magnetic field and surface temperature distribution. *A&A* 297, 441–450, 1995.
- Zavlin, V.E. Theory of radiative transfer in neutron star atmospheres and its applications. In: Becker, W. (Ed.), *Neutron Stars and Pulsars* (Proceedings of the 363. WE-Heraeus Seminar), Springer, New York, pp. 181–211, 2009.